HHS Public Access

Author manuscript

Acta Biomater. Author manuscript; available in PMC 2018 August 01.

Published in final edited form as:

Acta Biomater. 2017 August ; 58: 421–431. doi:10.1016/j.actbio.2017.05.061.

A Multi-defense Strategy: Enhancing Bactericidal Activity of a Medical Grade Polymer with a Nitric Oxide Donor and Surface-immobilized Quaternary Ammonium Compound

Jitendra Pant[a,¥], **Jing Gao**[b,¥], **Marcus J. Goudie**[a], **Sean Hopkins**[a], **Jason Locklin**[a,b,*], and **Hitesh Handa**[a,*]

[a]School of Chemical, Materials and Biomedical Engineering, College of Engineering, University of Georgia, Athens, GA, USA

[b]Department of Chemistry, University of Georgia, Athens, GA, USA

Abstract

Although the use of biomedical devices in hospital-based care is inevitable, unfortunately, it is also one of the leading causes of the nosocomial infections, and thus demands development of novel antimicrobial materials for medical device fabrication. In the current study, a multi-defense mechanism against Gram-positive and Gram-negative bacteria is demonstrated by combining a NO releasing agent with a quaternary ammonium antimicrobial that can be covalently grafted to medical devices. Antibacterial polymeric com posites were fabricated by incorporating a nitric oxide (NO) donor, *S*-nitroso-*N*-acetyl-penicillamine (SNAP) in CarboSil® polymer and top coated with surface immobilized benzophenone based quaternary ammonium antimicrobial (BPAM) small molecule. The results suggest that SNAP and BPAM have a different degree of toxicity towards Gram-positive and Gram-negative bacteria, and the SNAP-BPAM combination is effective in reducing both types of adhered viable bacteria equally well. SNAP-BPAM combinations reduced the adhered viable *Pseudomonas aeruginosa* by 99.0% and *Staphylococcus aureus* by 99.98% as compared to the control CarboSil films. Agar diffusion tests demonstrate that the diffusive nature of NO kills bacteria beyond the direct point of contact which the non-leaching BPAM cannot achieve alone. This is important for potential application in biofilm eradication. The live-dead bacteria staining shows that the SNAP-BPAM combination has more attached dead bacteria (than live) as compared to the controls. The SNAP-BPAM films have increased hydrophilicity and higher NO flux as compared to the SNAP films useful for preventing blood protein and bacterial adhesion. Overall the combination of SNAP and BPAM imparts different attributes to the polymeric composite that can be used in the fabrication of antimicrobial surfaces for various medical device applications.

[*]Corresponding authors: Jason Locklin, Department of Chemistry, University of Georgia, 220 Riverbend Road, Athens, GA 30602, Telephone: (706) 542-2359, jlocklin@uga.edu; Hitesh Handa, School of Chemical, Materials and Biomedical Engineering, University of Georgia, 220 Riverbend Road, Athens, GA 30602, Telephone: (706) 542-8109, hhanda@uga.edu.

[¥]Both the authors contributed equally to this work

Graphical abstract

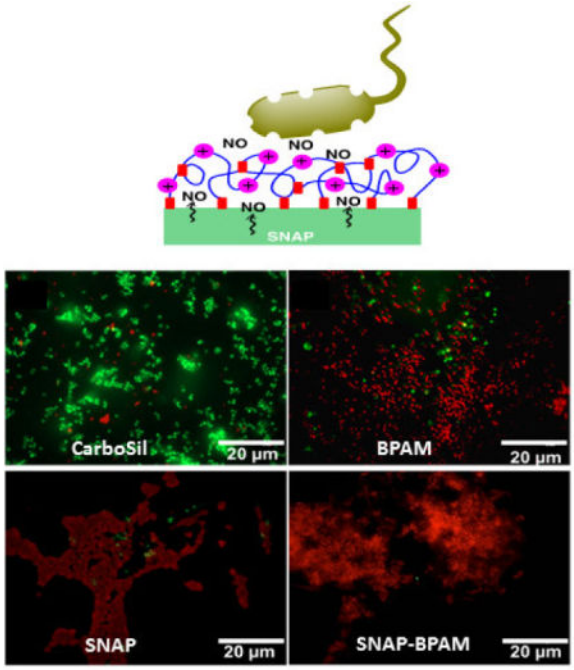

Keywords

Nitric oxide; SNAP; BPAM; quaternary ammonium; bacterial adhesion; biomedical device related infection

1. Introduction

Invasive medical devices predispose patients to more than 850,000 biomedical device-related infections (BDRIs) annually [1]. Out of various biomedical devices that are frequently used in clinical practices, intravenous infusion devices, and urinary catheters represent a major source of nosocomial septicemia [1, 2]. For instance, the incidences of catheter-related bloodstream infections in the United States are approximately 80,000 cases/year in intensive care units alone and up to 250,000 cases/year in total with an attributable mortality of up to 35% [3]. Medical devices or implants create high risks for infections through several modes including (i) infecting patients directly by serving as a substrate for microorganisms' growth and colonization (biofilm), and/or (ii) damaging or invading epithelial layer in the host, which is a barrier to infection. It is evident that incorporation of microbicides in the medical devices would prevent BDRIs and ultimately bring down the cost associated with prolonged hospital stays. Presently, antibiotics and silver nanoparticles-based approaches are used to kill microorganisms; however, the emergence of antibiotic resistance and the issue of cytotoxicity and genotoxicity raises alarming concerns [4–7]. Most of the BDRIs involve multiple strains of microorganisms, and hence treatment with a single antibiotic is not effective [8]. It has been shown that tolerance level for antibiotics is 1000 times higher for biofilms when compared to bacterial suspensions [9]. This demands immediate attention as

the use of multiple antibiotics and high doses only exacerbate the existing issues of antibiotic resistance and cytotoxicity. These challenges necessitate the exploration of alternative approaches to overcome the challenges of BDRIs caused by a wide variety of bacteria. In this regard, the combination of novel bactericidal agents such as surface-bound poly quaternary ammonium cations and nitric oxide (NO) donors can be advantageous due to their distinctive biocidal actions. This combination would not only assure high bactericidal efficiency but will also minimize the emergence of antibiotic resistance in pathogens due to their non-specific actions.

Membrane-disrupting poly “-onium” (quaternary ammonium) cations with various alkyl chain lengths have drawn considerable interest as a class of antimicrobial reagents because of their facile synthesis, broad application, outstanding antimicrobial activity, low cost, and low bacterial resistance [10–14]. Designing surfaces containing covalently bound poly “oniums” is one of the most successful strategies to date used to overcome surface microbial in fections [15–18]. Among these polycations, the benzophenone chromophore has been utilized to develop photochemically grafted quaternary ammonium coatings [19, 20]. Benzophenone based quaternary ammonium cations (BPAM) has been shown to exhibit instant contact killing and high biocidal activity against both Gram-positive and Gram-negative bacteria. BPAM also exhibits rapid surface attachment (within 1 min) to the polymer with mild UV irradiation and good mechanical durability (survives Taber abrasion testing) due to the high photochemical efficiency of benzophenone and cross-linked network structure with polymer post irradiation [20].

The generally accepted hypothesis for the biocidal mechanism of surface-immobilized quaternary ammoniums suggests that the positively charged “-onium” replaces the bacteria’s natural counterions (Mg^{2+} and Ca^{2+}) and disrupt the ionic integrity of the membrane [21, 22]. In addition, the alkyl chains of polycations intercalate into the phospholipid bilayer structure which disturbs its organization, forming holes in the membrane [23, 24]. An alternative mechanism bacteria killing by quaternary ammoniums hypothesized that phospholipids are drawn out of bacterial lipid bilayer where they can permeate into cationic films [25, 26]. Klibanov *et al.* have reported that bacteria fail to develop resistance to the lethal action of surface-bound quaternary ammonium because such surface acting antibacterial agent permeates bacterial membranes non-selectively via a ‘brute-force’ mechanism [11]. Although widely accepted as a highly efficient antibacterial agent, BPAM has several disadvantages that can limit its applications. The charge density of surface-bound quaternary ammonium might be eliminated by neutralization with anionic cellular components in the cytoplasm that is expelled out of the dead bacteria or screened by the layer of negatively charged dead bacterial cells covering the material’s surface [27, 28]. Moreover, due to its inability to act on bacteria that are not in intimate contact, BPAM cannot act on bacteria deeply embedded in a matrix of biofilm on a polymer surface. Furthermore, in the case of blood-contacting materials, fouling of the surface through the adsorption of protein can potentially hinder the surface-contact effect of quaternary ammonium cations such as BPAM on adhered bacteria. These limitations of the BPAM can be overcome by combining it with a nitric oxide (NO) donor as NO can diffuse through the biofilm matrix. Owing to its antimicrobial and antithrombotic potential, NO can provide antibacterial activity even if the surface of the material is compromised due to

aforementioned reasons [29, 30]. Schoenfisch group has done multiple studies demonstrating the combination of NO donors with other antimicrobials agents resulting in a significant improvement in the overall bactericidal activity of the material [31–33].

In nature, nitric oxide (NO) is an endogenously produced (macrophages, endothelial cells, neurons) free radical gas with a very short half-life of fewer than 5 seconds [34–39]. Healthy endothelium lining in the inner wall of blood vessels releases an estimated NO flux of 0.5 to 4.0×10^{-10} mol min^{-1} cm^{-2} [40–43]. Endogenous NO is catalytically released by nitric oxide synthase in mammals and plays an important role in the immune response to infections caused by bacteria, fungus or viruses [44, 45]. The NO released within the sinus cavities and macrophages functions as a natural antimicrobial agent to non-specifically combat pathogen invasion in mammals including humans [37]. Over the past two decades, NO-based therapies have emerged as a potential bactericidal agent to kill even the most prevalent pathogens causing hospital-acquired infection such as methicillin-resistant *Staphylococcus aureus* (MRSA) *and Pseudomonas aeruginosa*, and other bacteria including *Escherichia coli, Acinetobacter baumanii, Listeria monocytogenes*, and *Enterococcus faecalis* [29, 46–54]. The nonspecific innate immune response of NO results from lipid peroxidation and tyrosine nitration in the cell wall, nitrosation of amines and thiols in the extracellular matrix, and DNA cleavage in the cellular matrix [55]. Due to the non-specific action of NO and rapid reduction of bacteria load at the infection locale, the possibility of NO resistant strains remains limited [48, 52, 56–58]. In addition, NO based material can be used in blood-contacting device applications because it temporarily inhibits the activation of platelets on the polymer's surface which BPAM alone cannot [59]. The realization of the immense potential of NO in creating biomimetic materials has encouraged researchers to synthesize several NO donor molecules to allow the storage and local delivery of NO at the material surface. *S*-nitroso-*N* acetylpenicillamine (SNAP) is one such NO donor that has widely been used in developing NO-releasing materials [43, 52, 60–63]. In the past, Worley *et al.*, have demonstrated the (NO)-releasing quaternary ammonium (QA)-functionalized generation 1 (G1) and generation 4 (G4) poly(amidoamine) (PAMAM) dendrimers using *N*-diazonium diolate NO donors [32]. The present study demonstrates the enhanced bactericidal effect by permanent photocrosslinking and surface immobilization of BPAM on a CarboSil based polymeric composite with SNAP embedded as a NO donor.

This study investigated, the combined effect of the NO-releasing donor (SNAP) and nonleaching quaternary ammonium (BPAM) to prevent the adherence of bacterial cells on the polymeric surface in addition to killing bacteria beyond the direct point of contact. Briefly, polymeric films were prepared by incorporating SNAP in CarboSil® 20 80A (a medical grade silicone–polycarbonate-urethane copolymer). The BPAM was surface immobilized as a top-coat onto SNAP-CarboSil films by UV based photocrosslinking. The SNAP-BPAM based strategy to kill bacteria on the polymer surface was characterized physically and chemically and validated for its antibacterial efficiency.

2. Materials and Methods

2.1 Materials

CarboSil® 20 80A thermoplastic silicone–polycarbonate-urethane (hereafter will be referred to as CarboSil) was obtained from DSM Biomedical (Berkeley, CA). N-Acetyl-D-penicillamine (NAP), methanol, sodium chloride, potassium chloride, potassium phosphate monobasic, sodium phosphate dibasic, dimethylacetamide (DMAc), tetrahydrofuran (THF), ethylenediaminetetraacetic acid (EDTA), and sulfuric acid were obtained from Sigma-Aldrich (St. Louis, MO). N-Bromosuccinimide (NBS), 2, 2'-azo-bis(2-methylpropiontirle) (AIBN), and N, N-dimethyl dodecyl amine were purchased from Alfa-Aesar. LB broth, Lennox, and LB Agar, miller media were purchased from Fischer Bioreagents (Fair Lawn, NJ). 4-Methylbenzophenone (Oxchem), cyclohexane (Honeywell), that-amyl alcohol (JT Baker), isopropyl alcohol (IPA) (JT Baker) sodium chloride (EMD Chemical), and peptone (HiMedia) were used without further purification. Phosphate buffered saline (PBS), pH 7.4, containing 138mM NaCl, 2.7mM KCl, 10mM sodium phosphate, was used for all *in vitro* experiments including bacteria testing. The two-color fluorescent live/dead BacLight bacterial viability kit L7012 (Molecular Probes, Life Technologies) which contains SYTO® 9 green fluorescent nucleic acid stain and the propidium iodide red fluorescent nucleic acid stain was utilized to evaluate the bacterial viability. Gram- negative *Pseudomonas aeruginosa* (ATCC 27853) and Gram-positive *Staphylococcus aureus* (ATCC 6538) were originally obtained from American Type Tissue Collection (ATCC).

2.2 Instrumental Methods

UV-vis spectroscopy was performed on a Cary Bio Spectrophotometer (Varian). Two irradiation wavelengths, 254 and 365 nm, were utilized in this study. The UV light sources were a Compact UV lamp (UVP) and FB-UBXL-1000 UV Crosslinker (Fisher Scientific) with bulbs of 254 nm wavelength for small (1 × 1 cm) and larger (2.5 × 2.5 cm) substrates, respectively. The substrates were held at 0.5 cm from the light source during irradiation to obtain a power of 6.5 mW/cm^2. Another UV light source was an OmniCure, Series 1000 with 365 nm bandpass filter, equipped with a liquid-filled fiber optic waveguide. The polymeric composite films were held 2 cm from the source for a power of 25 mW/cm^2. The thickness of the surface grafted BPAM film was measured using an M-2000 spectroscopic ellipsometer (J.A. Woollam Co., Inc). Water contact angles were measured by a DSA 100 drop shape analysis system (KRŰSS) with a computer-controlled liquid dispensing system. Water droplets with a volume of 1 μL were used to measure the static contact angle. A fluorescent microscope (EVOS FL, Thermo-Scientific) equipped with a 100× objective was used for live/dead bacterial viability photomicrographs. A GFP FITC filter cube (excitation: 490 nm, emission: 503 nm) was used for SYTO® 9 and a Texas Red filter cube (excitation: 577 nm, emission: 620 nm) was used for the propidium iodide. The NO release study was performed using nitric oxide analyzer (NOA) 280i.

2.3 Synthesis of Bactericidal Agents and fabrication of polymeric films

2.3.1 *S*-Nitroso-*N*- acetylpenicillamine (SNAP) synthesis—A method reported by Chipinda et al. was modified for synthesizing SNAP from NAP [64]. Briefly, sodium nitrite and NAP were added in an equimolar ratio to a 1:1 mixture of methanol and water

containing 2 M H_2SO_4 and 2 M HCl. The mixture was stirred in the dark (to protect NO release by light stimulation) for 40 min using a magnetic stirrer. Thereafter, the reaction vessel was placed in an ice bath to precipitate the SNAP crystals. The resulting crystals were filtered out of the solution and allowed to air dry in dark followed by vacuuming to remove traces of any solvent. SNAP crystals were stored in a freezer prior to use.

2.3.2 Benzophenone based antimicrobial molecule (BPAM) synthesis—The benzophenone based antimicrobial molecule (BPAM) was prepared using the previously reported procedure of Gao et al., [20]. Briefly, 4-methylbenzopheone (6.0 g, 30.6 mM), NBS (6.0 g, 33.6 mM), AIBN (1.0 g, 6.1 mM), and cyclohexane (100 mL) were added to a round-bottom flask under nitrogen atmosphere. The suspension was stirred under reflux overnight. After stirring, the mixture was cooled and filtered to remove any solid residues and the filtrate was concentrated under reduced pressure. The solid mixture was dissolved in diethyl ether and washed with water, brine and dried over magnesium sulfate. The mixture was filtered and concentrated under reduced pressure. The recovered solid was recrystallized from absolute ethanol to give fine white crystals. Yield: 7.1 g, 89 %. ^{1}H NMR: δ, 7.80 (t, 2H, J = 3.0 Hz); 7.78 (t, 2H, J = 1.4 Hz); 7.60 (t, 1H, J = 7.0 Hz); 7.50 (d, 2H, 8.2 Hz); 7.49 (t, 2H, 7.6 Hz); 4.53 (s, 2H). ^{13}C NMR (CDCla): δ, 195.93, 142.09, 137.39, 132.54, 130.52, 129.99, 128.92 128.33, 128.16, 32.25.

N-(4-benzoylbenzyl)-N,N-dimethylbutan-1-aminium iodide (BPAM): (4-bromomethyl) benzophenone (1.7 g, 6.2 mM), N, N-demethyldodecylamine (1.7 mL, 6.2 mM), and tert-amyl alcohol (5 mL) were added to a sealable pressure flask. The mixture was stirred and heated in the sealed vessel at 95 °C for 24 h. The flask was cooled to room temperature and the solvent was removed under reduced pressure. The resulting brown waxy solid was recrystallized in hexane/ethyl acetate (7:4) to give a waxy white solid. Yield: 1.7 g, 67 %. ^{1}H NMR ($CDCl_3$): δ, 7.84 (dd, 4H, J = 8.2, 23.9 Hz); 7.75 (d, 2H, J = 7.0 Hz); 7.59 (t, 1H, J = 7.6 Hz); 7.47 (t, 2H, 7.7 Hz); 3.57 (m, 2H); 3.35 (s, 6H); 1.80 (bs, 2H); 1.31 (bs, 4H); 1.21 (bs, 16H); 0.84 (t, 3H, J= 6.6 Hz). ^{13}C NMR ($CDCl_3$): δ, 210.33, 139.75, 136.70, 133.53, 133.24, 131.53, 130.54, 130.24, 120.66, 66.63, 64.12, 49.85, 32.06, 29.69, 29.58, 29.46, 29.37, 26.42, 22.82, 14.29.

2.3.3 Fabrication of antimicrobial SNAP-CarboSil polymer films—To begin making the polymeric SNAP films, 70mg/mL of CarboSil was dissolved in tetrahydrofuran (THF) as a solvent and stirred for 1 h at room temperature using a magnetic stirrer. After complete dissolution, 10 % (w/w) of SNAP was quickly added and dissolved for 2 min in the Carbosil-THF solution. The SNAP films (10 wt %) were cast in Teflon molds (diameter = 2.5 cm) and dried overnight in dark to prevent undesired loss of NO from the films using 3 ml of resulting SNAP-CarboSil-THF solution. The films were coated twice with 50 mg/ml CarboSil solution (in THF). This outer coating ensures that SNAP does not leach out from the films and also generates a smooth surface. The control CarboSil films were prepared and coated in a similar manner, without the addition of SNAP.

2.3.4 Surface immobilization of BPAM on SNAP-CarboSil films—The BPAM film was immobilized onto SNAP-CarboSil film surfaces using spray coating. BPAM/ isopropanol solution (5 mg/mL) was sprayed using an airbrush spray gun from a distance of

20 cm onto a vertically placed substrate to achieve uniform coating. Upon solvent evaporation, a thin film of BPAM remained on the surface. Then BPAM coated films were subsequently irradiated with UV light (254 nm, 6.5 mW/cm^2) for 2 min to covalently immobilize BPAM to the surface. The films were sonicated with isopropanol for 1 min to rinse off any residual, physisorbed BPAM and dried under a stream of nitrogen. Figure 1 shows the fabrication procedure to make SNAP-BPAM CarboSil films (hereafter will be called SNAP-BPAM films).

2.4 Nitric Oxide release kinetics

Nitric oxide release from the SNAP and SNAP-BPAM films was measured using a Sievers Chemiluminescence Nitric Oxide Analyzer (NOA) 280i (Boulder, CO). The Sievers chemiluminescence NOA is considered as the gold standard for detecting *in vitro* nitric oxide release from the substrate. It is widely used for measurement of nitric oxide released from materials due to the ability to limit interfering species, such as nitrates and nitrites, as they are not transferred from the sample vessel to the reaction cell. Prior to NO release measurements, the films (n = 3) were incubated for 1 h (PBS containing 100 mM EDTA, room temperature) to avoid the burst release associated with NO-releasing materials [43, 61]. Films were then placed in the sample vessel immersed in PBS (pH 7.4) containing 100 mM EDTA. Nitric oxide was continuously purged from the buffer and swept from the headspace using nitrogen sweep gas and a bubbler into the chemiluminescence detection chamber. Films were submerged in PBS with EDTA and stored in glass vials and kept at 37°C between NO-release measurements. Fresh PBS solution was used for each NO-release measurement, and films were kept in fresh PBS solution for storage after each measurement.

2.5 UV-vis spectrophotometry

All UV-Vis spectra were recorded in the wavelength range of 200–700 nm using a UV-Vis spectrophotometer Cary Bio Spectrophotometer (Varian) at room temperature. CarboSil films and SNAP CarboSil films were developed on quartz glass substrates by spin coating with 200 μL of CarboSil/THF solution (50 mg/mL) at 1000 rpm for 30 s. BPAM was top coated on CarboSil/quartz substrates by spray coating with BPAM/IPA solution (10 mg/mL). The UV-vis spectrum of CarboSil was measured as the background. The presence of the S-NO group of SNAP provides characteristic absorbance maxima at 340 and 590 nm [43, 65]. CarboSil films were dissolved in DMAc and absorbance values were measured at 340 nm. The amount of SNAP was then determined using a calibration curve from known molar concentrations of SNAP in DMAC and compared to untreated control CarboSil films.

2.6 Quantification of adhered and viable colony forming units on polymeric surface

In this study, the ability of the CarboSil polymer with SNAP-BPAM combination to kill the adhered bacteria on the polymer surface was tested using the Gram-negative *Pseudomonas aeruginosa* and Gram-positive *Staphylococcus aureus* bacteria which are amongst the most common causes of hospital-acquired infections (HAIs). A modified protocol of standard bacterial adhesion tests was used to quantify the viable colony forming units of bacteria per surface area of the films (CFU/cm^2) [66–68]. A single colony of bacteria was isolated from a previously cultured LB-agar plate and incubated in LB medium for 14 h at 37°C at a rotating speed of 150 rpm. The optical density of the culture was measured at a wavelength of 600

nm ($O.D_{600}$) using UV-vis spectrophotometer (Thermo scientific Genesys 10S UV-Vis) to ensure that bacteria is in log phase of their growth. The bacteria culture was then centrifuged at 3500 rpm for 7 min, the supernatant was discarded. And sterile phosphate buffer saline (PBS), pH 7.4 was added to the bacterial pellet. This procedure was repeated twice to remove all traces of LB medium and to suspend bacteria in PBS solution. In parallel, serial dilutions of the bacteria were p repared and plated in LB agar Petri dishes in order to verify the consistency of concentration of viable cells between experiments. The OD_{600} of the cell suspension in PBS was measured and adjusted to the CFU/ml in the range of 10^7–10^9 based on the standard calibration curve. CarboSil control, SNAP films, BPAM coated CarboSil films and SNAP-BPAM films (n = 3 for each type; surface area = 0.94 cm^2) were exposed to bacterial cells (CFU: 10^7–10^9) at 37 °C for 24 h in a shaker incubator (150 rpm) after soaking them in PBS for 1 h to account for the burst effect. The 24 h incubation allows the bacteria to adhere to the surface of the films and the adhered bacteria were acted upon by BPAM and NO. After 24 h, films were removed from the solution and any loosely bound bacteria were washed by gently rinsing them with continuously flowing PBS (5 ml) using a pipette. The films were sonicated for 45 sec using an Omni-Tip homogenizer followed by vortexing for 30 seconds to collect the adhered bacteria into a 2 ml PBS solution. The PBS solution with bacteria was serially diluted (10^{-1}–10^{-5}), plated in the solid LB agar medium and incubated for 20 h at 37°C. After 20 h, the CFUs of the adhered viable bacteria on the surface of the polymer were counted keeping in account the dilution factor.

2.7 Analysis of residual NO flux post bacteria exposure

To ensure that fabricated film releases sufficient levels of nitric oxide after exposure to Pseudomonas *aeruginosa* or *Staphylococcus aureus strain* for 24 h (Section 2.6), the residual NO release was confirmed following the same procedure as explained in Section 2.4 using the Sievers Nitric Oxide Analyzer (NOA). Triplicates of each film types (n = 3) were analyzed for measuring the residual NO flux.

2.8 Zone of inhibition (ZOI) analysis

A standard agar diffusion protocol was followed to conduct zone of inhibition (ZOI) study to demonstrate the diffusive nature of NO molecule released from SNAP and SNAP-BPAM films in the surrounding agar. This study was designed to prove that the NO release from the polymeric composite can kill bacteria which are not in direct contact with the polymeric films which BPAM alone fails to achieve. As a proof of concept, Gram-positive *S. aureus* and Gram- negative *P. aeruginosa* bacteria strains were used for the study. A single colony of each bacterium was suspended individually in LB and incubated at 37°C for 14 h at a rotating speed of 150 rpm. Using *UV-Vis spectrophotometer* (Genesis 10S-Thermo Scientific), the optical density (OD) of each of the bacterial cultures was measured at 600 nm (OD_{600}). The observed OD_{600} was adjusted to 1×10^7 colony forming units per mL (CFUs/mL) based on a calibration curve based on the known concentration of *S. aureus* and *P. aeruginosa.* A sterile cotton swab was placed into each of the strain cultures and then gently pressed and rotated against premade LB-agar Petri dishes (14 cm) to spread the bacteria aseptically and uniformly. Circular disks (diameter: 22 mm) of control, SNAP, BPAM, and SNAP-BPAM films were placed on top of bacterial culture and pressed gently. The Petri dishes were incubated overnight at 37°C in inverted position. The ZOI diameters

were compared to evaluate the antimicrobial efficacy of NO releasing SNAP and SNAP-BPAM films.

2.9 Live/dead staining assay

While the bacterial adhesion test allows counting the viable CFUs on the surface of the polymer, it doesn't provide any quantitative or qualitative information on how many cells were initially attached and died due to SNAP-BPAM biocidal activity. Using live/dead staining, we observed both live and dead bacterial cells that were bound to the surface of the polymer. This qualitative study was then combined with Cell Profiler software to quantify the live and dead bacteria on the polymeric surface. SYTO® 9 dye, yields green fluorescence and labels all bacteria in a population with intact membranes. In contrast, propidium iodide, which yields red fluorescence, penetrates only the bacteria with damaged membranes and replaces SYTO® 9 stains, causing a reduction in green fluorescence and the appearance of red fluorescence. Consequently, bacteria with damaged cell membranes can be distinguished from live bacteria. For each of the bacterial strains, 10 mL bacterial culture was grown to late log phase in broth (shaken at 100 rpm for 10 h at 37 °C). The culture was centrifuged at 4000 rpm for 10 min. The supernatant was removed and the pellet was suspended in sterile distilled water. Before staining, 10 μL bacterial suspension with a concentration around 10^8 CFU/mL was placed on the CarboSil, BPAM coated CarboSil, SNAP-blended CarboSil, and SNAP-BPAM CarboSil films and dried at 37 °C for 5 min to achieve quick and intimate contact. Equal volumes of SYTO® 9 and propidium iodide (1.5 μL) were combined, added to 1 mL of distilled water, and mixed thoroughly. Diluted dye mixture (10 μL) was trapped between the slide with adhered bacteria and 18 mm square coverslip. The sample was incubated in dark for 15 min at room temperature and imaged qualitatively with an EVOS fluorescence microscope. Both the live and dead bacteria from the fluorescent images were then quantified with Cell Profiler software by randomly selecting different spots (n = 3) on the films.

2.10 Statistical significance

For all the quantitative measurements n = 3 data points were taken into consideration unless otherwise mentioned. Standard two-*tailed t*-test with unequal variance is used to do all statistical comparisons. The data is reported as a mean ± standard deviation and the significance with a p-value < 0.05 is stated for comparisons.

3. Results

3.1 Photocrosslinking of BPAM on SNAP-CarboSil and quantification of total SNAP

The benzophenone moiety of BPAM photochemically reacts with C-H groups of the CarboSil polymer to form new C-C bonds at the interface. Upon absorption of UV light, the promotion of one electron from a nonbinding n orbital to the antibonding π^* orbital of the carbonyl group yields a biradicaloid triplet state where the electron-deficient oxygen n orbital interacts with surrounding weak C-H δ bonds, resulting in H abstraction to complete the half-filled n orbital. The two resulting carbon radicals then combine to form a new C-C bond. This process was monitored by the decrease in absorbance of the n-π^* transition of BP using UV-vis spectrometry (Figure 2 (A)). Before exposure to UV light, the λ_{max}

absorbance at 255 nm was observed, which is the characteristic n-π^* transition of BPAM [20]. A spectrum shoulder ranging from 310–350 nm is assigned to the UV absorbance (λ_{max}) of SNAP [64]. The low intensity of the SNAP absorbance is due to the low concentration of SNAP within the CarboSil polymer matrix. After UV irradiation for 90 seconds, absorbance at 255 nm decreased, indicating the completion of the crosslinking reaction. The broad shoulder at 250~300 nm could be due to slight photo-oxidation of the polycarbonate base [69]. The remaining SNAP content after UV treatment is shown in Figure 2 (B) and was confirmed to maintain 95.44 ± 2.5% of the initial SNAP content. This can be mainly due to the presence of a top coat of Carbosil in the SNAP films before the application of BPAM. In the past, the application of top coats of CarboSil which are in the order of 100 microns has been shown to significantly reduce leaching when compared to non-top coated films [43]. These results confirmed that surface immobilized BPAM doesn't adversely cause significant loss of SNAP from the polymeric composite.

3.2 Nitric oxide release from SNAP and SNAP-BPAM CarboSil films

Incorporation of SNAP to CarboSil has shown to provide continuous and localized NO delivery to specific sites of interest [70, 71]. The incorporation of SNAP in medical grade polymers have been shown to be hemocompatible and possesses stability during long-term storage at room temperature and physiological conditions [63, 72, 73].

In this study, release rates of NO were measured at physiological conditions (pH 7.4, 37°C) to demonstrate that the presence of the BPAM coating does not adversely affect the NO release profile. The release of NO from these compounds stems from the breaking of the S-NO bond that can be catalyzed using heat, light, moisture, or metal ions [43, 60, 65]. Representative real-time NO release profiles from SNAP and SNAP-BPAM films was recorded via NOA as shown in Figure 3. SNAP films exhibited an initial release rate of 1.35 ± 0.11 × 10^{-10} mol min^{-1} cm^{-2} and release rate of 0.28 ± 0.02 × 10^{-10} mol min^{-1} cm^{-2} after 24 h. SNAP films with BPAM top coat showed an increase in NO flux both at the initial (2.58 ± 0.25 × 10^{-10} mol min^{-1} cm^{-2}) and at the 24-hour time point (0.59 ± 0.04 × 10^{-10} mol min^{-1} cm^{-2}) (Figure 4). This may be attributed to the increase in hydrophilicity of the films with the presence of BPAM topcoat as described above. The increased flux is still well within the physiological range (0.5–4.0 × 10^{-10} mol $min^{-1}cm^{-2}$) making it relevant and effective for biomedical device applications [40]. The NO flux exhibited by the films is sufficient to kill bacteria beyond 24 h. This has been shown *in vivo* in a 7-day sheep catheter model using similar hydrophobic polymers with 10 wt. % SNAP [74]. These materials exhibit similar NO release characteristics over a 28-d period and demonstrate that NO release rates at the lower end of physiological limits are still effective in providing antibacterial activity. Another report has also shown that hydrophobic polymers with SNAP have extended NO-release at physiological levels (up to 20 days) [70]. Furthermore, the incorporation of SNAP in medical grade polymers are not only hemocompatible and biocompatible but also stable during long-term storage (6 months) at room temperature [63, 72, 73].

3.3. Coating thickness and contact angle analysis

The coating thickness and static contact angle measurements are among the most relevant physical characterizations for a polymeric coating. The results of these characterizations are illustrated in Table 1. The thickness of the crosslinked BPAM coatings on CarboSil and SNAP CarboSil films after UV irradiation were 45.7 ± 0.3 nm and 47.9 ± 0.5 nm, respectively, indicating successful grafting of a BPAM coating. Water contact angles of control CarboSil, SNAP CarboSil, BPAM CarboSil, and SNAP-BPAM CarboSil surfaces are listed in Table 1. We have previously shown that due to lower water uptake of CarboSil, limited leaching of SNAP has been seen from SNAP doped CarboSil [71]. The study showed that leaching is further reduced with the use of a top coat as compared to the non-coated films. With addition of BPAM coat on top of the Carbosil topcoat no changes to the leaching kinetics of SNAP is expected.

Blending SNAP into the CarboSil polymeric matrix does not affect the hydrophobicity of the polymer. The CarboSil control surface was found to have a contact angle (CA) of 119.3 ± 0.4°. The surface grafted layer of BPAM significantly decreases the hydrophobicity of the CarboSil based polymer film, reducing the CA to 63.5° ± 0.5°, resulting from the positively charged ammonium functional groups. The increase in the surface hydrophilicity is expected to increase the antibacterial efficacy of the SNAP-BPAM polymer films as studies have shown a marked increase in NO release from the hydrophilic surface when compared to the hydrophobic surfaces [43]. This is in line with the results obtained from the NO release kinetics study (Section 3.2). Furthermore, increased hydrophilicity helps in the repulsion of non-specific protein adsorption, and ultimately bacterial adhesion [75, 76] as confirmed by the bacterial adhesion test (Section 3.4) and Live/Dead staining (Section 3.6).

3.4 Quantification of adhered viable bacteria (CFU/cm^2)

Biofilm formation is a major cause of morbidity and mortality associated with hospital acquired infection (HAIs). *Staphylococcus aureus*, a Gram-positive bacterium, and *Pseudomonas aeruginosa*, a Gram-negative bacterium are among the most common causes of nosocomial bloodstream infections that can form embedded biofilm matrices on indwelling biomedical devices [77–79]. As shown in Figure 5, the amount of viable *P. aeruginosa and S. aureus* adhered on SNAP-BPAM film surfaces are significantly lower than that of control films. While BPAM and SNAP are excellent antimicrobial agents, the combination offers several advantages not possessed by an individual antimicrobial agent. BPAM by itself has a superior antibacterial potential towards Gram-negative *P. aeruginosa* as compared to SNAP, and SNAP is superior with respect to its bactericidal action against Gram-positive *S. aureus*. The combination is very effective against both Gram-positive and negative bacteria. Overall the SNAP-BPAM films significantly reduced the adhered viable bacteria (both Grams positive and negative) as compared to the control films. SNAP-BPAM films showed a 4-log reduction in Gram-positive *S. aureus* and 3-log reduction for Gram-negative *P. aeruginosa* as compared to the CarboSil control. Figure 5 and Table 2 represents the respective graphs and the data for the reduction in the adhered CFU of both the bacteria per surface area of the polymeric composites. The difference in the results between the two bacteria can be attributed to the difference in the cell wall and membrane composition of Gram-positive and Gram-negative bacteria [80].

Non-leaching BPAM can only act on bacteria in intimate contact while NO can act beyond the direct point of contact because of diffusion. The activity of BPAM is also diminished with time by the layer of bacterial cells (live or dead) on polymeric composites as they tend to neutralize the charge on quaternary ammonium. This problem can be addressed by the application of NO. The small molecular size of NO allows it to diffuse through the bacterial biofilm and kill the bacterial cells which are otherwise resistant to bactericidal agents [53, 54]. In other words, the gradually released NO extended the life of BPAM by lowering the concentration of surrounding bacteria near the surface. The SNAP-BPAM films have relatively higher hydrophilicity (due to BPAM coat) than SNAP films alone which increased the NO flux release from the SNAP-BPAM films.

The residual NO analysis after exposing films to bacteria suspension (Figure 6) showed an abundance of NO up to $0.92 \pm 0.05 \times 10^{-10}$ mol min^{-1} cm^{-2} flux, suggesting that these films can continue to exhibit antibacterial properties beyond 24 h. The combined action of these bactericidal agents via multiple mechanisms of bacteria killing warrants a significant reduction in viable bacterial load for both Gram-positive and negative strains.

3.5 Bacterial killing via NO diffusion

While BPAM is an excellent antimicrobial agent, due to its non-diffusive nature, it cannot kill the bacteria protected within the biofilm matrix. Moreover, the charge density of surface-bound BPAM might be neutralized with anionic cellular components in the cytoplasm that is expelled out of the dead bacteria or screened by the layer of negatively charged dead bacterial cells covering the material's surface [26–28]. Therefore, the diffusive nature of NO can be beneficial in biofilm eradication beyond the close vicinity of the material which otherwise can't be achieved via BPAM application. The standard agar diffusion test allowed us to show the bactericidal effect of the NO releasing films in the presence and absence of the BPAM.

The CarboSil films with incorporated antimicrobial agents (SNAP-BPAM) and their combination resulted in a zone of inhibition (ZOI) of different diameters when exposed to LB agar plates with bacterial culture. As expected, the result demonstrated that BPAM has no ZOI, while the SNAP films and SNAP-BPAM films showed a clear ZOI due to the release of NO gas from SNAP when placed in an incubator at 37°C for 20 h (Figure 7). The explanation for this is the diffusive nature of NO that can penetrate in the LB agar and hence prevent the bacterial growth in the area around the film. The breaking of the S-NO bond in SNAP causes the release of NO. On the other hand, BPAM is non-diffusive in nature and hence can only act on bacteria which are in direct contact. From an application point of view, this can be beneficial for biofilm eradication as NO due to its small size would easily penetrate through the matrix of a bacterial biofilm. Even though BPAM didn't show any ZOI, it did prevent the growth of bacteria in direct contact underneath the film. The ZOI for *P. aeruginosa* was observed to be 24 mm for SNAP films and 26mm for SNAP-BPAM films. Similarly, the ZOI for S. *aureus* was observed to be 24 mm with SNAP films and 25 mm for SNAP-BPAM films. Overall SNAP-BPAM composites showed the largest ZOI for both S. *aureus* as well as *P. aeruginosa* strains among all the composites. The bigger ZOI with SNAP-BPAM combination is due to increase in NO flux with BPAM topcoat ($1.35 \pm 0.11 \times$

10^{-10} in SNAP films vs $2.58 \pm 0.25 \times 10^{-10}$ mol min^{-1} cm^{-2} in SNAP-BPAM films) as observed by chemiluminescence NOA. Figure 7 shows the comparative ZOI diameter among the films for both the bacterial strains. The difference in antibacterial efficacy shown towards the two bacterial strains can be attributed to the membrane properties of Gram-positive and Gram-negative bacteria [80].

3.6 Analysis and quantitation of live/dead stain test on CarboSil films

As mentioned above, the bacterial adhesion test (section 3.4) showed the reduction in adhered viable cells and zone of inhibition agar diffusion test (section 3.5) demonstrated the killing of bacteria through diffusion respectively. However, the relative number of live and dead bacteria on the films were not evaluated by either of these tests. Therefore, the antibacterial activity of the SNAP-BPAM hybrid CarboSil films was also evaluated using a live/dead fluorescent stain assay which stains the live cells as green and the dead cells as red. Figure 8 shows fluorescent images of S. *aureus* cells exposed on control CarboSil, BPAM, SNAP, and SNAP-BPAM films. The bacterial cell count for the live/dead assay was quantitatively estimated at three randomly selected spots on polymeric composites by using Cell Profiler software as recommended by published reports [81, 82]. On the control films (Figure 8A), 97.35 ± 0.72 % bacterial cells showed green fluorescence, evenly distributed across the surface, and retained intact spherical shape, suggesting that the tested bacterial cells were viable. On BPAM coated CarboSil films (Figure 8B), 94.41 ± 0.61 % of the total bacterial cells were stained red, indicating the cell membrane disruption caused by contact with surface-bound quaternary ammonium. On SNAP films, 97.58 ± 0.44 % of the total bacteria showed red fluorescence indicating dead cells (Figure 8C). In the case of SNAP-BPAM CarboSil films (Figure 8D), a 99.62 ± 0.59 % killing efficacy was achieved, demonstrating that the hybrid method effectively enhances the antibacterial activity of the functionalized biocompatible polymer material. This enhancement in bactericidal activity of SNAP-BPAM as compared to SNAP and BPAM films is in line with the viable bacteria adhesion test as well as the zone of inhibition testing. Notably, the pattern of aggregation of bacterial cells on the surface of the film was observed to be different and dependent on the antibacterial agent. The bacterial cells on control CarboSil and BPAM films have a regular pattern of bacterial cell distribution. On the other hand, the cells were aggregated together with irregular and distorted morphologies on SNAP Carbosil films, possibly due to the hydrophobicity of the CarboSil surface which caused repulsion to the negatively charged bacterial cells. On the SNAP-BPAM films, the dead cells with distorted morphologies (like that of SNAP films) were dispersed across the surface which might be due to the relatively lower hydrophobicity (C.A = 63.5° ± 0.5) of the SNAP-BPAM films' surface as compared to SNAP films (C.A = 115° ± 0.2) resulting from the positively charged ammonium functional groups. Such distortion and irregularity in bacterial colonies can also be attributed to the deterioration of bacterial cell wall by NO as observed via Atomic Electron Microscopy and Cell Surface Topography analysis [83]. Overall, lived/dead staining experiment combined with Cell Profiler software further validated that combined NO and surface-bound quaternary ammonium can provide dual antibacterial activities and thus significantly enhance the biocidal activity as compared to the individual agent. The authors suggest further *in vitro* testing and high-resolution image analysis on bacterial aggregation pattern to validate this plausible theoretical explanation.

4. Discussion

In the present study, an NO donor molecule (SNAP) and a surface immobilized benzophenone based antimicrobial molecule (BPAM) were used in combination and their combined effect to reduce microbial adhesion and viability on a medical grade polymeric surface was evaluated. Since the λ_{max} of BPAM and SNAP are distinctly separated, this benefits the hybrid material in two ways: (1) BPAM can absorb photons efficiently for the photoreaction even in the presence of SNAP; (2) Photo-degradation of SNAP is limited in the crosslinking process since the irradiation wavelength is 254 nm for the maximum energy absorbance efficiency of BPAM.

The antibacterial potential of SNAP-BPAM films was tested via (i) Bacterial adhesion test (ii) Agar diffusion test (iii) Live/Dead staining. All these three tests allowed to quantitatively assess the bacterial adhesion (both viable and non-viable) and their subsequent killing by NO and BPAM action. The antimicrobial properties of NO are due to denaturation of enzymes, deamination of DNA and lipid oxidation in bacteria matrix [55]. On the other hand, BPAM kills the bacteria in direct contact by damaging the bacterial cell membrane integrity due to electrostatic interactions [21, 22].

In the past, we have shown that SNAP based NO releasing polymers have many desirable properties from a translational perspective such as the long-term storage stability (6 months), ease of sterilization, and extended NO release (> 2 weeks) without negatively affecting the physical characteristics, bacterial inhibition, biocompatibility, and hemocompatibility of the polymer [43, 53, 62, 63]. Similarly, the surface grafted BPAM has been reported to exhibit excellent antimicrobial activity against Gram-positive and Gram-negative bacteria on instant contact due to high surface charge density of the deposited BPAM thin film [20]. However, this is the first study that combines SNAP and BPAM to demonstrate their antibacterial potential.

The study demonstrated that the SNAP-BPAM combination has better antibacterial properties than SNAP or BPAM alone. BPAM is highly regarded as a bactericidal agent, but, it can only act on bacteria that are in direct contact. NO molecule through its diffusive nature allows acting on bacteria that are beyond the direct contact. This property is useful to act on biofilm matrix that otherwise prevents the penetration of antibacterial agent and keeps the bacteria immune. BPAM however, imparts a relatively hydrophilic surface to SNAP-CarboSil as apparent from a decrease in the contact angle. Studies have shown higher NO release from the hydrophilic surface when compared to the hydrophobic surfaces which in turn resulted in higher bacterial killing [43]. This is in accordance with the NO flux analysis as the SNAP-BPAM films showed higher NO flux as compared to the SNAP only films. Furthermore, a hydrophilic surface helps in the repulsion of non-specific protein adsorption, and ultimately bacterial adhesion [75, 76] as confirmed by the bacterial adhesion test and Live/Dead staining. From a translational perspective, a biomedical implant fabricated with a non-leaching, hydrophilic surface would be able to form a solvated, aqueous layer upon contact with body fluids and thus reduce bacterial adhesion [84].

In vitro characterization of the SNAP-BPAM containing CarboSil polymer in the present showed that such polymeric composites can yield better antibacterial effect as compared to SNAP or BPAM individually (Figures 5, 7, and 8). Their distinct but very effective mode of bactericidal action assures that the bacteria that in contact with the polymeric composites are attacked via multiple bactericidal mechanisms. The NO release with the SNAP-BPAM combination was shown to be higher than with SNAP alone making their cooperation more effective in terms of diffusion of NO into the biofilm (Figures 3 and 4). These SNAP-BPAM- CarboSil composites continued to release NO flux in the physiological range past the bacteria exposure for 24 h (Figure 6). The sustained release of diffusible NO also extended the duration of localized action of BPAM by lowering the concentration of surrounding viable bacteria near the polymer surface allowing BPAM to kill any bacteria in local contact.

Overall, the combined action of these bactericidal agents via distinct mechanisms warrants a significant reduction in viable bacterial load for both Gram-positive and negative strains. Furthermore, the rapid action of NO (half-life < 5sec) and non-specific lethal action of surface-bound BPAM via physical membrane disruption limit the development of resistant bacterial strains [48, 52, 56–58].

5. Conclusion

In the current study, a polymeric composite was fabricated by blending SNAP in the CarboSil polymer and BPAM was surface grafted via UV photocrosslinking and its ability to inhibit bacteria on the surface was tested both qualitatively and quantitatively. The SNAP-BPAM combination was more effective in maximizing the bacterial load on the surface of the polymeric composite as compared to SNAP or BPAM films individually. The bacterial adhesion test demonstrated that combination is equally effective in minimizing the adhered viable CFUs of both Gram-positive and Gram-negative bacteria whereas SNAP was more effective against *S. aureus* and BPAM alone was more effective against *P. aureginosa* when tested alone. As demonstrated by the agar diffusion test diffusive nature of NO allowed to kill the bacteria beyond the direct point of contact which BPAM can't achieve alone. This is important for potential application in biofilm eradication. The lived dead staining allowed to observe that SNAP-BPAM combination has a higher number of attached dead bacteria (than live) with irregular morpohogies as compared to the controls. BPAM coat also increased the hydrophilicity and resulted in higher NO flux as compared to the SNAP only films. Overall, all these characteristics are ideal for controlling biomedical device related infections, especially in preventing bacteria from developing antibiotic resistance due to the different killing mechanisms exhibited by SNAP and BPAM. Such highly effective antimicrobial attributes offer a new paradigm in the fabrication of antimicrobial surfaces for various medical device applications.

Acknowledgments

Funding for this work was supported by National Institutes of Health, USA grants K25HL111213, R01HL134899, and Centers for Disease Control and Prevention contract 200-2016-91933.

References

1. STAMM WE. Infections related to medical devices. Annals of Internal Medicine. 1978; 89(5_Part_2):764–769. [PubMed: 717950]
2. Brisbois EJ, Kim M, Wang X, Mohammed A, Major TC, Wu J, Brownstein J, Xi C, Handa H, Bartlett RH. Improved Hemocompatibility of Multilumen Catheters via Nitric Oxide (NO) Release from S-Nitroso-N-acetylpenicillamine (SNAP) Composite Filled Lumen. ACS Appl Mater Interfaces. 2016; 8(43):29270–29279. [PubMed: 27734679]
3. Warren JW. Catheter-associated urinary tract infections. Infectious disease clinics of North America. 1997; 11(3):609–622. [PubMed: 9378926]
4. Stewart PS, Costerton JW. Antibiotic resistance of bacteria in biofilms. The lancet. 2001; 358(9276): 135–138.
5. Lee YH, Cheng FY, Chiu HW, Tsai JC, Fang CY, Chen CW, Wang YJ. Cytotoxicity, oxidative stress, apoptosis and the autophagic effects of silver nanoparticles in mouse embryonic fibroblasts. Biomaterials. 2014; 35(16):4706–4715. [PubMed: 24630838]
6. Park EJ, Yi J, Kim Y, Choi K, Park K. Silver nanoparticles induce cytotoxicity by a Trojan-horse type mechanism. Toxicol In Vitro. 2010; 24(3):872–878. [PubMed: 19969064]
7. AshaRani P, Low Kah Mun G, Hande MP, Valiyaveettil S. Cytotoxicity and genotoxicity of silver nanoparticles in human cells. ACS nano. 2008; 3(2):279–290.
8. Raad I, Darouiche R, Hachem R, Sacilowski M, Bodey GP. Antibiotics and prevention of microbial colonization of catheters. Antimicrobial agents and chemotherapy. 1995; 39(11):2397–2400. [PubMed: 8585715]
9. Jefferson KK, Goldmann DA, Pier GB. Use of confocal microscopy to analyze the rate of vancomycin penetration through Staphylococcus aureus biofilms. Antimicrobial agents and chemotherapy. 2005; 49(6):2467–2473. [PubMed: 15917548]
10. Yatvin J, Gao J, Locklin J. Durable Defense: Robust and Varied Attachment of Non-leaching Poly"-Onium" Bactericidal Coatings to Reactive and Inert Surfaces. Chemical Communications. 2014; 50(67):9433–9442. [PubMed: 24882521]
11. Milović NM, Wang J, Lewis K, Klibanov AM. Immobilized N-Alkylated Polyethylenimine Avidly Kills Bacteria by Rupturing Cell Membranes with No Resistance Developed. Biotechnology and Bioengineering. 2005; 90(6):715–722. [PubMed: 15803464]
12. Yudovin-Farber I, Beyth N, Nyska A, Weiss EI, Golenser J, Domb AJ. Surface Characterization and Biocompatibility of Restorative Resin Containing Nanoparticles. Biomacromolecules. 2008; 9(11):3044–3050. [PubMed: 18821794]
13. Koplin SA, Lin S, Domanski T. Evaluation of the Antimicrobial Activity of Cationic Polyethylenimines on Dry surfaces. Biotechnology Progress. 2008; 24(5) 116021165.
14. Ferreira L, Zumbuehl A. Non-leaching Surfaces Capable of Killing Microorganisms on Contact. Journal of Materials Chemistry. 2009; 19(42):7796–7806.
15. Park D, Wang J, Klibanov AM. One-Step, Painting-Like Coating Procedures To Make Surfaces Highly and Permanently Bactericidal. Biotechnology Progress. 2006; 22(2):584–589. [PubMed: 16599580]
16. Xie Y, Hill CAS, Xiao Z, Militz H, Mai C. Silane coupling agents used for natural fiber/polymer composites: A review. Composites Part A: Applied Science and Manufacturing. 2010; 41(7):806–819.
17. Yuan SJ, Pehkonen SO, Ting YP, Neoh KG, Kang ET. Inorganic-Organic Hybrid Coatings on Stainless Steel by Layer-by-Layer Deposition and Surface-Initiated Atom-Transfer-Radical Polymerization for Combating Biocorrosion. ACS Applied Materials & Interfaces. 2009; 1(3): 640–652. [PubMed: 20355986]
18. Locklin JJ. US Pat. 2013
19. Dhende VP, Samanta S, Jones DM, Hardin IR, Locklin J. One-Step Photochemical Synthesis of Permanent, Nonleaching, Ultrathin Antimicrobial Coatings for Textiles and Plastics. ACS Applied Materials & Interfaces. 2011; 3(8):2830–2837. [PubMed: 21692449]

20. Gao J, Huddleston NE, White EM, Pant J, Handa H, Locklin J. Surface Grafted Antimicrobial Polymer Networks with High Abrasion Resistance. ACS Biomaterials Science & Engineering. 2016
21. Kügler R, Bouloussa O, Rondelez F. Evidence of A Charge-Density Threshold for Optimum Efficiency of Biocidal Cationic Surfaces. Microbiology. 2005; 151(5):1341–1348. [PubMed: 15870444]
22. Sonenshein AL, Hoch JA, Losick R. Bacillus Subtilis and Other Gram-positive Bacteria: Biochemistry, Physiology, and Molecular Genetics. American Society for Microbiology. 1993
23. Lewis K, Klibanov AM. Surpassing Nature: Rational Design of Sterile-Surface Materials. Trends in Biotechnology. 2005; 23(7):343–348. [PubMed: 15922467]
24. Tiller, JC. Antimicrobial Surfaces. In: Borner, HG., Lutz, JF., editors. Bioactive Surfaces. 2011. p. 193-217.
25. Bieser AM, Tiller JC. Mechanistic Considerations on Contact-Active Antimicrobial Surfaces with Controlled Functional Group Densities. Macromolecular bioscience. 2011; 11(4):526–534. [PubMed: 21229579]
26. Gao J, White EM, Liu Q, Locklin J. Evidence for the Phospholipid Sponge Effect as the Biocidal Mechanism in Surface-Bound Polyquaternary Ammonium Coatings with Variable Cross-Linking Density. ACS Appl Mater Interfaces. 2017; 9(8):7745–7751. [PubMed: 28145683]
27. Bieser AM, Tiller JC. Mechanistic Considerations on Contact-Active Antimicrobial Surfaces with Controlled Functional Group Densities. Macromolecular Bioscience. 2011; 11(4):526–534. [PubMed: 21229579]
28. Lee SB, Koepsel RR, Morley SW, Matyjaszewski K, Sun Y, Russell AJ. Permanent, Nonleaching Antibacterial Surfaces. 1. Synthesis by Atom Transfer Radical Polymerization. Biomacromolecules. 2004; 5(3):877–882. [PubMed: 15132676]
29. Nablo BJ, Prichard HL, Butler RD, Klitzman B, Schoenfisch MH. Inhibition of implant-associated infections via nitric oxide release. Biomaterials. 2005; 26(34):6984–6990. [PubMed: 15978663]
30. Carpenter AW, Schoenfisch MH. Nitric oxide release: Part II. Therapeutic applications. Chem Soc Rev. 2012; 41(10):3742–3752. [PubMed: 22362384]
31. Carpenter AW, Worley BV, Slomberg DL, Schoenfisch MH. Dual action antimicrobials: nitric oxide release from quaternary ammonium-functionalized silica nanoparticles. Biomacromolecules. 2012; 13(10):3334–3342. [PubMed: 22998760]
32. Worley BV, Slomberg DL, Schoenfisch MH. Nitric oxide-releasing quaternary ammonium-modified poly (amidoamine) dendrimers as dual action antibacterial agents. Bioconj Chem. 2014; 25(5):918–927.
33. Worley BV, Schilly KM, Schoenfisch MH. Anti-biofilm efficacy of dual-action nitric oxide-releasing alkyl chain modified poly (amidoamine) dendrimers. Mol Pharm. 2015; 12(5):1573–1583. [PubMed: 25873449]
34. Hou Y, Janczuk A, Wang P. Current trends in the development of nitric oxide donors. Current Pharmaceutical Design. 1999; 5(6):417–442. [PubMed: 10390607]
35. Vodovotz Y, Bogdan C, Paik J, Xie Q, Nathan C. Mechanisms of suppression of macrophage nitric oxide release by transforming growth factor beta. The Journal of experimental medicine. 1993; 178(2):605–613. [PubMed: 7688028]
36. Hibbs JB, Taintor RR, Vavrin Z, Rachlin EM. Nitric oxide: a cytotoxic activated macrophage effector molecule. Biochem Biophys Res Commun. 1988; 157(1):87–94. [PubMed: 3196352]
37. MacMicking J, Xie Q-w, Nathan C. Nitric oxide and macrophage function. Annu Rev Immunol. 1997; 15(1):323–350. [PubMed: 9143691]
38. Halpenny GM, Heilman B, Mascharak PK. Nitric Oxide (NO)-Induced Death of Gram- negative Bacteria from a Light Controlled NO-Releasing Platform. Chemistry & Biodiversity. 2012; 9(9): 1829–1839. [PubMed: 22976973]
39. Rouby JJ. The nose, nitric oxide, and paranasal sinuses: the outpost of pulmonary antiinfectious defenses? American Journal of Respiratory and Critical Care Medicine. 2003; 168(3):265–266. [PubMed: 12888602]
40. Vaughn MW, Kuo L, Liao JC. Estimation of nitric oxide production and reactionrates in tissue by use of a mathematical model. Am J Physiol: Heart Circ Physiol. 1998; 274(6):H2163–H2176.

41. Handa H, Brisbois EJ, Major TC, Refahiyat L, Amoako KA, Annich GM, Bartlett RH, Meyerhoff ME. In vitro and in vivo study of sustained nitric oxide release coating using diazeniumdiolate-doped poly (vinyl chloride) matrix with poly (lactide-co-glycolide) additive. Journal of Materials Chemistry B. 2013; 1(29):3578–3587.
42. Handa H, Major TC, Brisbois EJ, Amoako KA, Meyerhoff ME, Bartlett RH. Hemocompatibility comparison of biomedical grade polymers using rabbit thrombogenicity model for preparing nonthrombogenic nitric oxide releasing surfaces. J Mater Chem B. 2014; 2(8):1059–1067.
43. Brisbois EJ, Handa H, Major TC, Bartlett RH, Meyerhoff ME. Long-term nitric oxide release and elevated temperature stability with S-nitroso-N-acetylpenicillamine (SNAP)-doped Elast-eon E2As polymer. Biomaterials. 2013; 34(28):6957–6966. [PubMed: 23777908]
44. DeGroote MA, Fang FC. Antimicrobial properties of nitric oxide. Nitric oxide and infection, Springer. 2002:231–261.
45. Pant, J., Goudie, M., Brisbois, E., Handa, H. Advances in Polyurethane Biomaterials. Elsevier; 2016. Nitric oxide releasing polyurethanes; p. 471-550.
46. Sundaram J, Pant J, Goudie MJ, Mani S, Handa H. Antimicrobial and Physicochemical Characterization of Biodegradable, Nitric Oxide-Releasing Nanocellulose-Chitosan Packaging Membranes. J Agric Food Chem. 2016
47. Brisbois EJ, Bayliss J, Wu J, Major TC, Xi C, Wang SC, Bartlett RH, Handa H, Meyerhoff ME. Optimized polymeric film-based nitric oxide delivery inhibits bacterial growth in a mouse burn wound model. Acta Biomater. 2014; 10(10):4136–4142. [PubMed: 24980058]
48. Heilman BJ, Halpenny GM, Mascharak PK. Synthesis, characterization, and light-controlled antibiotic application of a composite material derived from polyurethane and silica xerogel with embedded photoactive manganese nitrosyl. Journal of Biomedical Materials Research Part B: Applied Biomaterials. 2011; 99(2):328–337.
49. Nablo BJ, Chen TY, Schoenfisch MH. Sol-gel derived nitric-oxide releasing materials that reduce bacterial adhesion. J Am Chem Soc. 2001; 123(39):9712–9713. [PubMed: 11572708]
50. Nablo BJ, Schoenfisch MH. Antibacterial properties of nitric oxide-releasing sol-gels. Journal of Biomedical Materials Research Part A. 2003; 67(4):1276–1283. [PubMed: 14624514]
51. Hetrick EM, Schoenfisch MH. Reducing implant-related infections: active release strategies. Chem Soc Rev. 2006; 35(9):780–789. [PubMed: 16936926]
52. Hetrick EM, Schoenfisch MH. Antibacterial nitric oxide-releasing xerogels: Cell viability and parallel plate flow cell adhesion studies. Biomaterials. 2007; 28(11):1948–1956. [PubMed: 17240444]
53. Pant J, Goudie MJ, Hopkins SP, Brisbois EJ, Handa H. Tunable nitric oxide release from S-nitroso-N-acetylpenicillamine via catalytic copper nanoparticles for biomedical applications. ACS Appl Mater Interfaces.
54. Singha P, Pant J, Goudie MJ, Workman CD, Handa H. Enhanced antibacterial efficacy of nitric oxide releasing thermoplastic polyurethanes with antifouling hydrophilic topcoats. Biomaterials Science. 2017
55. Fang FC. Perspectives series: host/pathogen interactions. Mechanisms of nitric oxide- related antimicrobial activity. Journal of Clinical Investigation. 1997; 99(12):2818–2825. [PubMed: 9185502]
56. Privett BJ, Broadnax AD, Bauman SJ, Riccio DA, Schoenfisch MH. Examination of bacterial resistance to exogenous nitric oxide. Nitric Oxide. 2012; 26(3):169–173. [PubMed: 22349019]
57. Feelisch M. The use of nitric oxide donors in pharmacological studies. Naunyn- Schmiedeberg's Arch Pharmacol. 1998; 358(1):113–122. [PubMed: 9721012]
58. Bogdan C. Nitric oxide and the immune response. Nat Immunol. 2001; 2(10):907–916. [PubMed: 11577346]
59. Hakim T, Sugimori K, Camporesi E, Anderson G. Half-life of nitric oxide in aqueous solutions with and without haemoglobin. Physiological measurement. 1996; 17(4):267. [PubMed: 8953625]
60. Williams DLH. The chemistry of S-nitrosothiols. Accounts of Chemical Research. 1999; 32(10): 869–876.
61. Brisbois EJ, Major TC, Goudie MJ, Bartlett RH, Meyerhoff ME, Handa H. Improved hemocompatibility of silicone rubber extracorporeal tubing via solvent swelling-impregnation of

S-nitroso-N-acetylpenicillamine (SNAP) and evaluation in rabbit thrombogenicity model. Acta biomaterialia. 2016; 37:111–119. [PubMed: 27095484]

62. Brisbois EJ, Davis RP, Jones AM, Major TC, Bartlett RH, Meyerhoff ME, Handa H. Reduction in thrombosis and bacterial adhesion with 7 day implantation of S-nitroso-N-acetylpenicillamine (SNAP)-doped Elast-eon E2As catheters in sheep. Journal of Materials Chemistry B. 2015
63. Goudie MJ, Brisbois EJ, Pant J, Thompson A, Potkay JA, Handa H. Characterization of an S-nitroso-N-acetylpenicillamine–based nitric oxide releasing polymer from a translational perspective. Int J Polym Mater Polym Biomater. 2016; 65(15):769–778.
64. Chipinda I, Simoyi RH. Formation and stability of a nitric oxide donor: S-nitroso-N-acetylpenicillamine. The Journal of Physical Chemistry B. 2006; 110(10):5052–5061. [PubMed: 16526748]
65. Frost MC, Meyerhoff ME. Controlled photoinitiated release of nitric oxide from polymer films containing S-nitroso-N-acetyl-DL-penicillamine derivatized fumed silica filler. J Am Chem Soc. 2004; 126(5):1348–1349. [PubMed: 14759186]
66. Nablo BJ, Schoenfisch MH. Poly (vinyl chloride)-coated sol– gels for studying the effects of nitric oxide release on bacterial adhesion. Biomacromolecules. 2004; 5(5):2034–2041. [PubMed: 15360321]
67. Nablo BJ, Rothrock AR, Schoenfisch MH. Nitric oxide-releasing sol–gels as antibacterial coatings for orthopedic implants. Biomaterials. 2005; 26(8):917–924. [PubMed: 15353203]
68. Torres N, Oh S, Appleford M, Dean DD, Jorgensen JH, Ong JL, Agrawal CM, Mani G. Stability of antibacterial self-assembled monolayers on hydroxyapatite. Acta Biomater. 2010; 6(8):3242–3255. [PubMed: 20188873]
69. Diepens M, Gijsman P. Photo-oxidative degradation of bisphenol A polycarbonate and its possible initiation processes. Polymer Degradation and Stability. 2008; 93(7):1383–1388.
70. Wo Y, Li Z, Brisbois EJ, Colletta A, Wu J, Major TC, Xi C, Bartlett RH, Matzger AJ, Meyerhoff ME. Origin of long-term storage stability and nitric oxide release behavior of carbosil polymer doped with S-nitroso-N-acetyl-D-penicillamine. ACS Appl Mater Interfaces. 2015; 7(40):22218–22227. [PubMed: 26393943]
71. Goudie MJ, Brainard BM, Schmiedt CW, Handa H. Characterization and in vivo performance of nitric oxide-releasing extracorporeal circuits in a feline model of thrombogenicity. Journal of Biomedical Materials Research Part A. 2016
72. Brisbois EJ, Major TC, Goudie MJ, Meyerhoff ME, Bartlett RH, Handa H. Attenuation of thrombosis and bacterial infection using dual function nitric oxide releasing central venous catheters in a 9day rabbit model. Acta Biomater. 2016; 44:304–312. [PubMed: 27506125]
73. Brisbois EJ, Kim M, Wang X, Mohammed A, Major TC, Wu J, Brownstein J, Xi C, Handa H, Bartlett RH. Improved Hemocompatibility of Multi-Lumen Catheters via Nitric Oxide (NO) Release from S-Nitroso-N-acetylpenicillamine (SNAP) Composite Filled Lumen. ACS Appl Mater & Interfaces. 2016
74. Brisbois EJ, Davis RP, Jones AM, Major TC, Bartlett RH, Meyerhoff ME, Handa H. Reduction in thrombosis and bacterial adhesion with 7 day implantation of S-nitroso-N-acetylpenicillamine (SNAP)-doped Elast-eon E2As catheters in sheep. J Mater Chem B. 2015; 3(8):1639–1645.
75. Rana D, Matsuura T. Surface Modifications for Antifouling Membranes. Chem Rev. 2010; 110:2448–2471. [PubMed: 20095575]
76. Chen S, Li L, Zhao C, Zheng J. Surface hydration: Principles and applications toward low-fouling/nonfouling biomaterials. Polymer. 2010; 51(23):5283–5293.
77. Allan ND, Giare-Patel K, Olson ME. An in vivo rabbit model for the evaluation of antimicrobial peripherally inserted central catheter to reduce microbial migration and colonization as compared to an uncoated PICC. BioMed Research International. 2012; 2012
78. Otto M. Staphylococcal infections: mechanisms of biofilm maturation and detachment as critical determinants of pathogenicity. Annu Rev Med. 2013; 64:175–188. [PubMed: 22906361]
79. Kiedrowski MR, Horswill AR. New approaches for treating staphylococcal biofilm infections. Annals of the New York Academy of Sciences. 2011; 1241(1):104–121. [PubMed: 22191529]
80. Roy H. Tuning the properties of the bacterial membrane with aminoacylated phosphatidylglycerol. IUBMB life. 2009; 61(10):940–953. [PubMed: 19787708]

81. Carpenter AE, Jones TR, Lamprecht MR, Clarke C, Kang IH, Friman O, Guertin DA, Chang JH, Lindquist RA, Moffat J, Golland P, Sabatini DM. CellProfiler: image analysis software for identifying and quantifying cell phenotypes. Genome Biology. 2006; 7(10):1–11.

82. Kamentsky L, Jones TR, Fraser A, Bray MA, Logan DJ, Madden KL, Ljosa V, Rueden C, Eliceiri KW, Carpenter AE. Improved structure, function and compatibility for CellProfiler: modular high-throughput image analysis software. Bioinformatics. 2011; 27(8):1179–1180. [PubMed: 21349861]

83. Deupree SM, Schoenfisch MH. Morphological analysis of the antimicrobial action of nitric oxide on Gram-negative pathogens using atomic force microscopy. Acta Biomater. 2009; 5(5):1405–1415. [PubMed: 19250890]

84. Louie JS, Pinnau I, Ciobanu I, Ishida KP, Ng A, Reinhard M. Effects of polyether-polyamide block copolymer coating on performance and fouling of reverse osmosis membranes. Journal of Membrane Science. 2006; 280(1–2):762–770.

Statement of Significance

A significant increase in the biomedical device related infections (BDRIs), inability of the currently existing antimicrobial strategies to combat them and a proportional rise in the associated morbidity demands development of novel antimicrobial surfaces. Some of the major challenges associated with the currently used therapeutics are: antibiotic resistance and cytotoxicity. In the current study, engineered polymeric composites with multi-defense mechanism were fabricated to kill bacteria via both active and passive mode. This was done by incorporating a nitric oxide (NO) donor *S*-nitroso-*N*-acetypenicillamine (SNAP) in a medical grade polymer (CarboSil®) and a benzophenone based quaternary ammonium antimicrobial small molecule (BPAM) was surface immobilized as the top layer. The developed biomaterial was tested with Gram-positive and Gram-negative strains and was found to be effective against both the strains resulting in up to 99.98% reduction in viable bacterial count. This preventative strategy can be used to fabricate implantable biomedical devices (such as catheters, stents, extracorporeal circuits) to not only significantly limit biofilm formation but also to reduce the antibiotic dose which are usually given post infections.

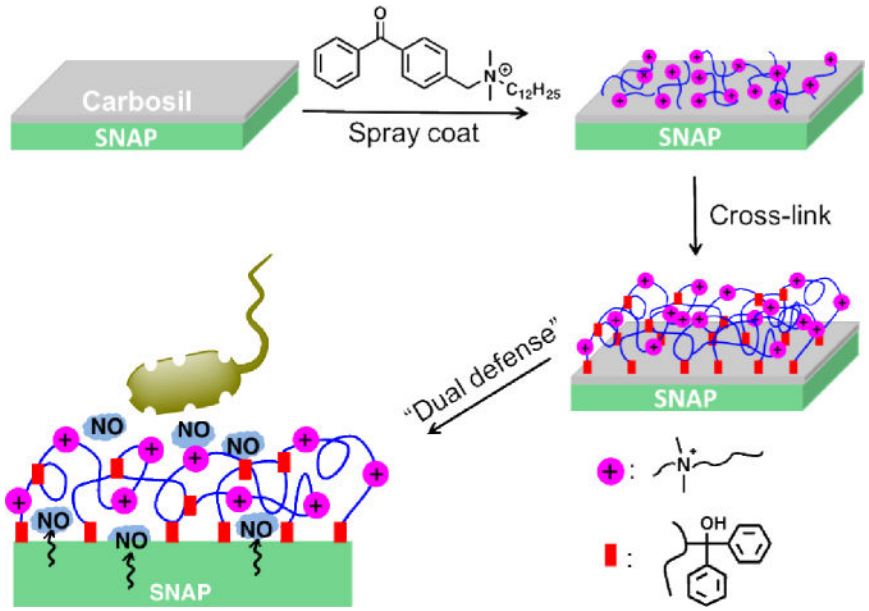

Figure 1.

The fabrication of the SNAP-BPAM CarboSil film and its biocidal action. Antibacterial polymeric composites were fabricated by incorporating a NO donor, *S*-nitroso-*N*-acetyl-penicillamine (SNAP) in CarboSil polymer and top coated with surface immobilized benzophenone based quaternary ammonium antimicrobial (BPAM) small molecule via photocrosslinking.

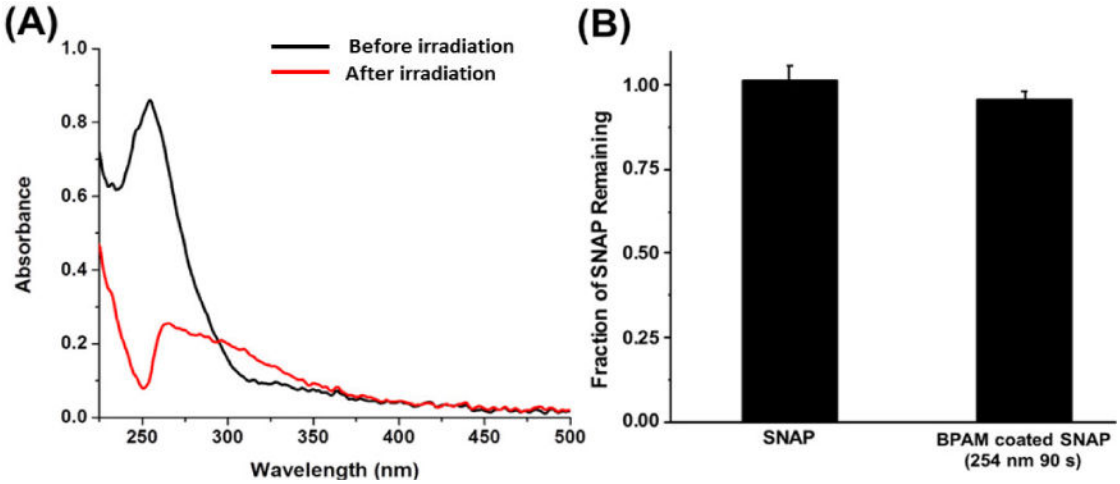

Figure 2.

UV-mediated photocrosslinking study of BPAM on SNAP film: (A) UV-Vis Spectra of SNAP-BPAM film before and after UV irradiation (254 nm, 90 s). After UV irradiation for 90 seconds, absorbance at 255 nm decreased, indicating the completion of the crosslinking reaction. (B) Total SNAP content after UV irradiation was reported to be approximately 95.44 ± 2.5% of the initial SNAP content. The data is reported as a mean ± standard deviation for n=3 samples and the significance with a p-value < 0.05 is stated for comparisons.

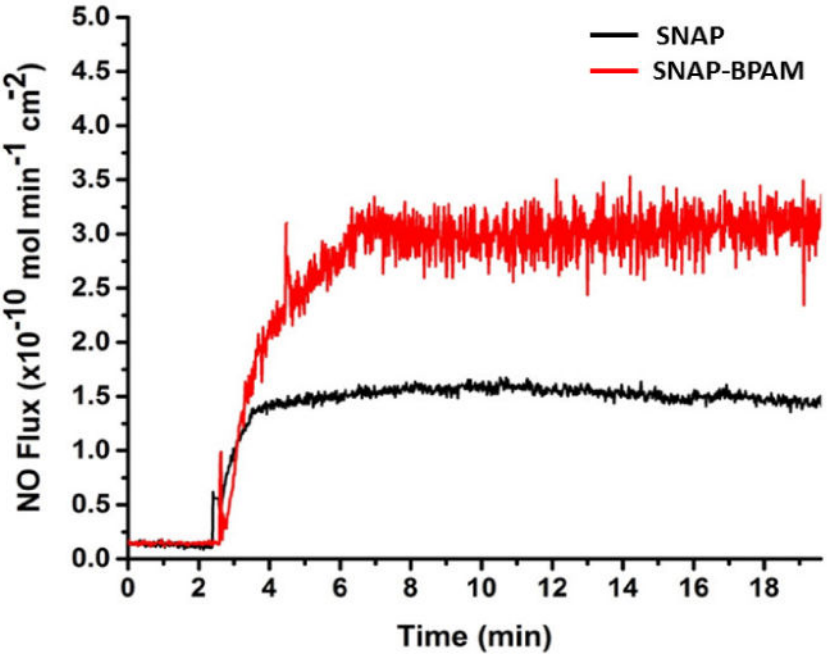

Figure 3.

Real-time NO flux rate of SNAP doped CarboSil (black) and BPAM coated SNAP CarboSil films (red) analyzed at the physiological temperature using Sievers Nitric Oxide Analyzer (NOA).

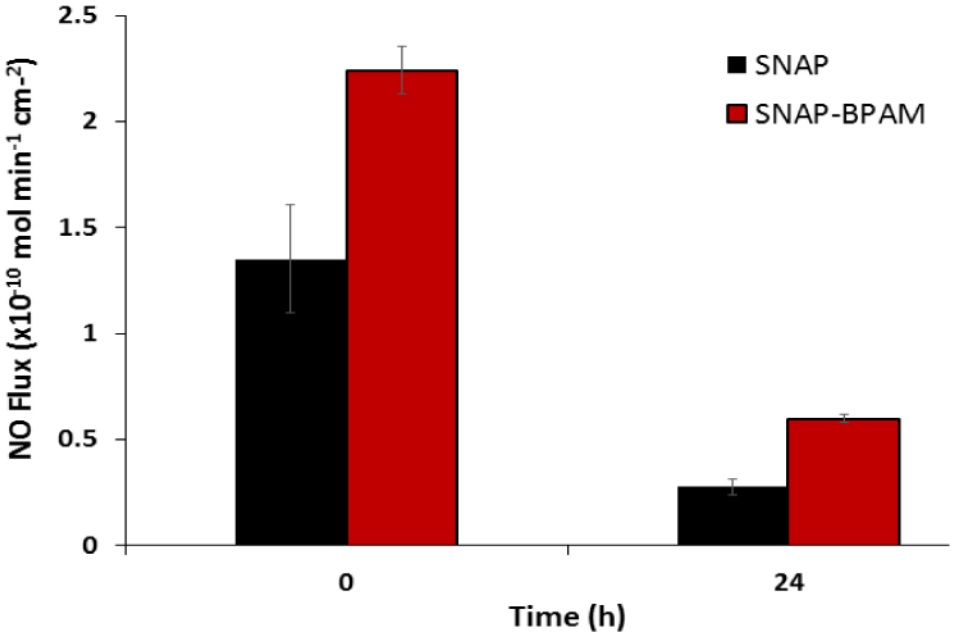

Figure 4.

Nitric oxide (NO) flux analysis of SNAP and SNAP-BPAM films (at 0h and 24h time-period). The SNAP-BPAM films released higher NO flux at initially and at 24 h time point. The NO flux of SNAP-BPAM was maintained in the physiological range even after 24 h. The data is reported as a mean ± standard deviation for n=3 samples and the significance with a p-value < 0.05 is stated for comparisons.

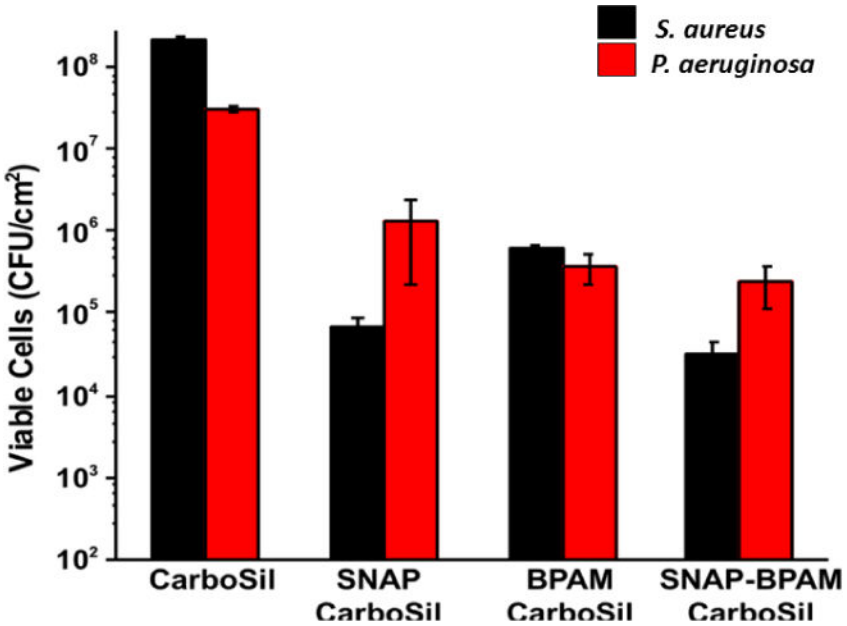

Figure 5.

Comparative graphs to show the differences in inhibition of viable colony forming units of Gram-positive S. *aureus* and Gram-negative *P. aeruginosa* on the unit surface area (CFU/cm^2) of SNAP films, BPAM films and SNAP-BPAM films as compared to control CarboSil. The results suggest that both SNAP and BPAM has different degree of toxicity towards gram positive and negative bacteria. While BPAM by itself has better antibacterial potential towards gram negative *P. aeruginosa* as compared to SNAP, SNAP is better than BPAM w.r.t its bactericidal action against gram positive S. *aureus.* The combined action of SNAP-BPAM works equally well against both the bacteria. The data is reported as a mean ± standard deviation for n=3 samples and the significance with a p-value < 0.05 is stated for comparisons.

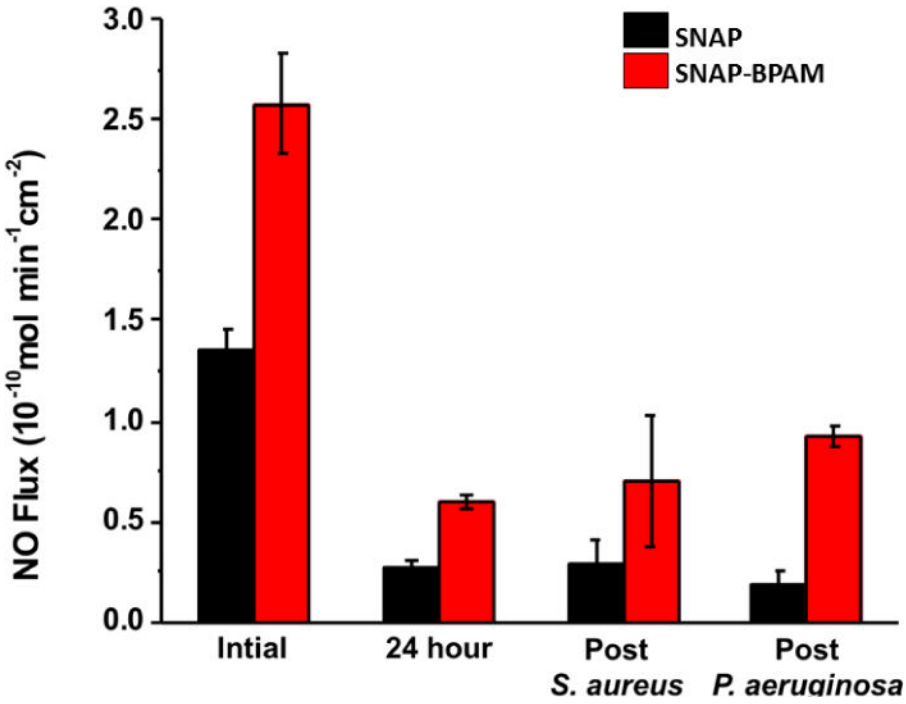

Figure 6.

Effect of immobilized BPAM top coats on NO release kinetics of the SNAP-BPAM films as measured by chemiluminescence before (0h and 24h) and after bacterial exposure (24h study). The residual NO flux was observed to be in the physiological range even after 24h of bacteria exposure indicating the antibacterial effect can be extended beyond the 24h. The data is reported as a mean ± standard deviation for n=3 samples and the significance with a p-value < 0.05 is stated for comparisons.

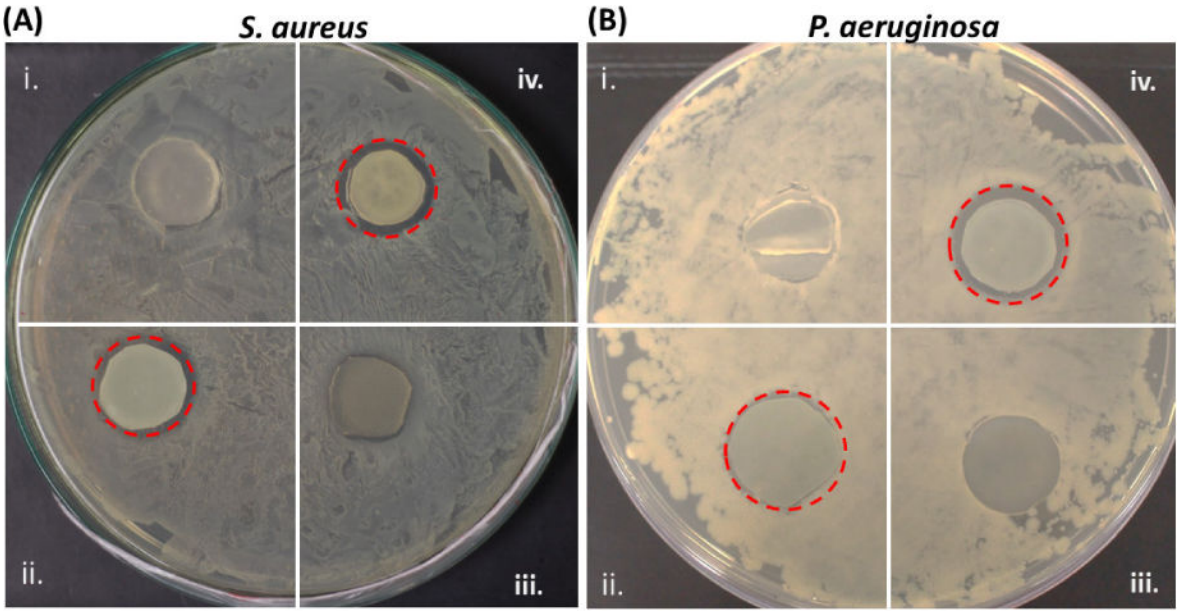

Figure 7.

Zone of inhibition (ZOI) can be seen inside the dotted red circle: (A) *S. aureus*; (B) *P. aeruginosa*; (i) Control, (ii) SNAP, (iii) BPAM, and (iv) SNAP-BPAM. The bigger ZOI with SNAP-BPAM combination is due to increase in NO flux with BPAM topcoat.

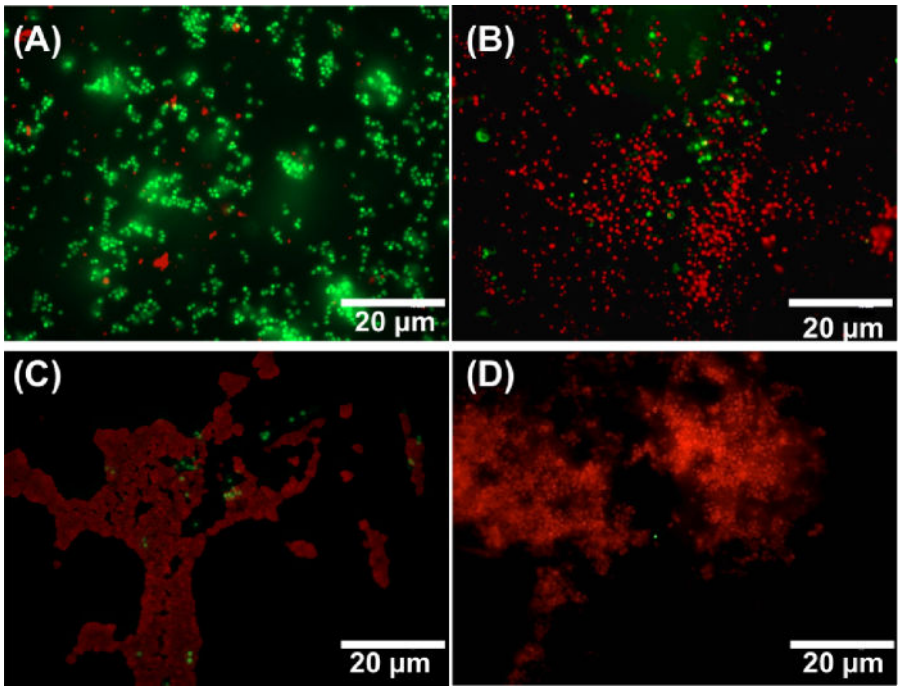

Figure 8.

Representative fluorescent images of *S. aureus* in contact with (A) Control CarboSil film, (B) BPAM film, (C) SNAP film and (D) SNAP-BPAM film after live-dead staining observed fluorescence microscopy. The red color indicates dead cells while the green fluorescence indicates viable bacteria. Using the Cell Profiler software, 97.35 ± 0.72 % of the total bacterial cells were observed to be viable (green florescence) on control films (A). On BPAM films (B), 94.41 ± 0.61 % bacterial cells were stained red, indicating the cell membrane disruption caused by contact with surface-bound quaternary ammonium. On SNAP film (C), 97.58 ± 0.44 % bacteria were dead (red fluorescence). In the case of SNAP-BPAM film (D), 99.62 ± 0.59 % of the total cells were dead (red fluorescence), demonstrating that the hybrid method effectively enhances the antibacterial activity of the functionalized biocompatible polymer material. As obvious from the image, SNAP-BPAM combination (D) showed the maximum bactericidal efficiency. The data is reported as a mean ± standard deviation for n=3 image from each sample type are considered for analysis.

Table 1

Physical properties of antibacterial SNAP-BPAM film.

Sample	CarboSil	SNAP CarboSil	BPAM CarboSil	SNAP-BPAM CarboSil
Thickness (nm)	N/A	N/A	45.7 ± 0.3	47.9 ± 0.5
Contact Angle (°)	119.3 ± 0.4	115 ± 0.2	67.9 ± 0.6	63.5 ± 0.5

The data is reported as a mean ± standard deviation for n=3 samples and the significance with a p-value < 0.05 is stated for comparisons.

Table 2

A comparative viable bacterial adhesion data for polymeric composites and NO flux analysis before and after bacterial exposure.

Films	NO flux* (0h)	NO flux* (24h)	*S. aureus* (CFU/cm^2)	*P. aeruginosa* (CFU/cm^2)	Residual NO flux* Post *S.A*	Residual NO flux* Post *P.A*
Carbosil	–	–	$2.1 \times 10^8 \pm 7.3 \times 10^6$	$3.0 \times 10^8 \pm 9.7 \times 10^5$	–	
BPAM	–	–	6.0 × 105 ± 5.9 × 104	3.8 × 105 ± 6.2 × 104	–	
SNAP	1.35 ± 0.11	0.28 ± 0.02	6.6 × 104 ± 2.0 × 104	1.3 × 106 ± 5.9 × 105	0.19 ± 0.07	0.30 ± 0.12
SNAP-BPAM	2.21 ± 0.25	0.35 ± 0.04	3.0 × 104 ± 7.0 × 103	2.3 × 105 ± 8.3 × 104	0.70 ± 0.32	0.92 ± 0.06

The data is reported as a mean ± standard deviation for n=3 samples and the significance with a p-value < 0.05 is stated for comparisons. Post S. *A* indicates NO flux after 24h of S. *aureus* exposure and post *P. A* indicates NO flux after 24h of *P. aeruginosa* exposure.

*NO flux ($\times 10^{-10}$ mol min^{-1}cm^{-2}).